Analysis of Nonuniform Nonlinear Distributed Feedback Structures Using a Simple Numerical Approach

Chu-Sheng Yang, Yen-Chung Chiang, and Hung-Chun Chang, *Senior Member, IEEE*

***Abstract*—A simple numerical approach previously proposed for calculating the input-intensity dependence of the reflectivity and transmissivity of a nonlinear dielectric slab for incident plane electromagnetic waves is adopted for analyzing nonuniform nonlinear distributed feedback (NLDFB) structures. The method is first validated by checking with the analytic solution for the bistability characteristics of a strictly periodic, uniform NLDFB structure as well as the reported transmission characteristics of linear structures based on transfer matrix method calculation. The method is then applied to determine the transmission bistability characteristics of linearly tapered and linearly chirped NLDFB structures. The results are found to be different in some cases from those based on a generalized transfer matrix calculation in which the nonuniform structure is approximated by a set of strictly periodic, uniform segments.**

***Index Terms*—Bistability devices, nonlinear distributed feedback structures, nonlinear gratings, optical waveguide gratings.**

I. Introduction

NONLINEAR distributed feedback (NLDFB) structures have been an important optical structure which attracts much interest in such applications as optical switching, limiting, bistability and multistability, and pulse shaping. Their properties have been theoretically studied [1], [2] and experimentally demonstrated [3]–[5]. In this paper we consider nonuniform NLDFB structures, in particular, tapered and chirped structures. One application of the tapered and chirped structure was to increase the excitation efficiency of nonlinear waveguide devices [6]. Although the continuous-wave optical response of a strictly periodic NLDFB structure has been derived analytically in terms of Jacobian elliptic functions by Winful *et al.* [2], the response of a general nonuniform NLDFB structure can only be obtained using the numerical approach. Radic *et al.* [7] proposed a generalized transfer matrix method for analyzing nonuniform NLDFB structures, which divided the nonuniform structure into a set of strictly periodic segments, with the transfer matrix of each segment readily obtainable based on Winful's analytic result. As in [1], *Radic et al.* considered one-dimensional (1-D) problem by assuming that the DFB structure is uniform in the transverse plane.

One of the present authors proposed a simple numerical approach for calculating the input-intensity dependence of the reflectivity and transmissivity of a nonlinear dielectric slab for both transverse-electric (TE) and transverse-magnetic (TM) obliquely incident plane electromagnetic waves [8] when others were employing complicated analysis methods. Only a set of first-order differential equations derived from Maxwell's equations needs to be solved, and most importantly, the problem was substantially simplified as being solved "backward," i.e., assuming first a known transmitted wave and then determining the corresponding reflected and incident waves from the calculated fields at the interface on the incident side. In such manner the input-intensity dependent reflectivity and transmissivity can be easily obtained. Radic *et al.* [7] also made use of the backward solution idea so that iterative solution procedure could be avoided. The solution method of [8] is readily applicable to a slab medium having arbitrary inhomogeneity transverse to its interface in the linear permittivity distribution and arbitrary nonlinearity with the permittivity depending on the electric field of the wave in the slab. Therefore, it can be used to solve the 1-D nonuniform NLDFB structure in a numerically *exact* manner, compared to the *approximate* method of [7] due to the employment of the nonuniform-structure segmentation. In this study we only consider the normally incident wave and the analysis using the method of [8] can be further simplified.

The simple numerical technique will be described in Section II. Numerical examples are given in Section III for comparison with those in [2] and [7]. The conclusion is drawn in Section IV.

II. Numerical Approach

Consider the problem shown in Fig. 1. An arbitrary 1-D NLDFB structure of thickness L is located between two linear dielectric regions 1 and 3 with uniform refractive index n_0. We assume that the material system is uniform in the transverse $(x-y)$ plane and the permeability in all three regions is μ_0, that of free space. A uniform plane wave with electric field in the y-direction and angular frequency ω is normally incident from region 1 onto the nonuniform NLDFB structure. The expression for the incident electric field in region 1 is written as

$$\mathbf{E_i}(z) = \hat{y}E_{i0}\exp\left[-j(\beta_i z - \phi_i)\right] \tag{1}$$

Manuscript received February 2, 2004; revised April 16, 2004. This work was supported in part by the National Science Council, R.O.C., under Grant NSC90-2215-E002-028 and Grant NSC91-2215-E002-031.

C.-S. Yang is with the Department of Electrical Engineering, National Taiwan University, Taipei, Taiwan 106-17, R.O.C.

Y.-C. Chiang was with the Department of Electrical Engineering, National Taiwan University, Taipei, Taiwan 106-17, R.O.C. He is now with VIA Technologies Inc., Taipei 231, Taiwan, R.O.C.

H.-C. Chang is with the Department of Electrical Engineering, the Graduate Institute of Electro-Optical Engineering, and the Graduate Institute of Communication Engineering, National Taiwan University, Taipei, Taiwan 106-17, R.O.C.

Digital Object Identifier 10.1109/JQE.2004.833209

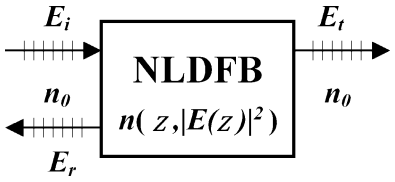

Fig. 1. Sketch of the problem considered: a uniform plane wave is normally incident onto an NLDFB structure of thickness L with nonuniform linear perturbation profile.

where $\beta_i = n_0\omega\sqrt{\mu_0\epsilon_0}$ with ϵ_0 being the permittivity of free space, E_{i0} is the real amplitude, and ϕ_i is a constant phase. For the reflected and transmitted electric fields, the expressions are the same except that the subscript i is replaced by r and t, respectively, and $-j$ by j for the reflected wave. We assume $\phi_i = 0$ and leave ϕ_r and ϕ_t unknown. In the nonlinear region 2 the electric field is expressed as $\hat{y}\tilde{E}_{2y}(z)$.

Kerr-like nonlinear medium is considered for region 2 where the permittivity is dependent on the local intensity of the wave, expressed as

$$\epsilon\left(z, \left|\tilde{E}_{2y}(z)\right|\right) = \epsilon_0\left[\epsilon_{rL}(z) + n_0 n^{(2)}\left|\tilde{E}_{2y}(z)\right|^2\right] \quad (2)$$

where $n^{(2)}$ is the effective Kerr index and $\epsilon_{rL}(z) = n_L^2(z)$ is the linear relative permittivity which describes the arbitrary z-dependent nonuniformity. In this paper we consider the sinusoidal type grating with

$$n_L(z) = n_0 + n_1(z)\cos\left[2\beta_B(z)z\right] \quad (3)$$

where n_0 corresponds to the uniform part and $n_1(z)$ represents the perturbation of the linear refractive index. Note that under the assumptions of the nonlinear coupled-mode theory (CMT), both the index perturbation $n_1(z)$ and the Bragg wavenumber $\beta_B(z)$ are slowly varying functions of z. Our formulation eliminates these restrictions from an NLDFB structure, and thus is a powerful method for dealing with various cases such as NLDFB structures of arbitrary index profile and extremely short length.

From Maxwell's equations, we have the following relations for the fields in the nonlinear region 2 with the real and imaginary parts of the fields separated [8]

$$\frac{\partial}{\partial z}\mathrm{Re}\left[\tilde{E}_{2y}(z)\right] = -\beta_0\eta_0\mathrm{Im}\left[\tilde{H}_{2x}(z)\right] \quad (4)$$

$$\frac{\partial}{\partial z}\mathrm{Im}\left[\tilde{E}_{2y}(z)\right] = \beta_0\eta_0\mathrm{Re}\left[\tilde{H}_{2x}(z)\right] \quad (5)$$

$$\frac{\partial}{\partial z}\mathrm{Re}\left[\tilde{H}_{2x}(z)\right] = -\frac{\beta_0}{\eta_0}\left(\frac{\epsilon}{\epsilon_0}\right)\mathrm{Im}\left[\tilde{E}_{2y}(z)\right] \quad (6)$$

$$\frac{\partial}{\partial z}\mathrm{Im}\left[\tilde{H}_{2x}(z)\right] = \frac{\beta_0}{\eta_0}\left(\frac{\epsilon}{\epsilon_0}\right)\mathrm{Re}\left[\tilde{E}_{2y}(z)\right] \quad (7)$$

where the subscript x or y denotes the component of the corresponding field, $\beta_0 = \omega(\mu_0\epsilon_0)^{1/2}$, and $\eta_0 = (\mu_0/\epsilon_0)^{1/2}$ is the intrinsic impedance of free space.

Since only the transmitted wave travels in region 3, we can solve the problem in a backward manner [8]. Assuming that the amplitude of the transmitted field is known and leaving the constant phase ϕ_t out of the transmitted field, we have $\tilde{E}_{2y}$ and $\tilde{H}_{2x}$ at $z = L$ by the continuity boundary conditions. Then, by integrating (4)–(7) numerically using the fourth-order Runge–Kutta method, the fields $\tilde{E}_{2y}$ and $\tilde{H}_{2x}$ can be obtained everywhere within the NLDFB structure. Once $\tilde{E}_{2y}$ and $\tilde{H}_{2x}$ are acquired at $z = 0$, from the boundary conditions at $z = 0$

$$E_{i0}\exp(-j\phi_t) + E_{r0}\exp\left[j(-\phi_t + \phi_r)\right] = \tilde{E}_{2y}(0) \quad (8)$$

$$-\frac{\beta_1}{\omega\mu_0}E_{i0}\exp(-j\phi_t) + \frac{\beta_1}{\omega\mu_0}E_{r0}\exp\left[j(-\phi_t + \phi_r)\right] = \tilde{H}_{2x}(0). \quad (9)$$

E_{i0}, E_{r0}, ϕ_r, and ϕ_r can be easily determined and the transmissivity and reflectivity $|T|^2 = |E_{t0}/E_{i0}|^2$ and $|\Gamma|^2 = |E_{r0}/E_{i0}|^2$ can be calculated. If we apply similar treatment at points within the NLDFB structure, we can also obtain the forward and backward traveling fields $E_+(z)\exp(j\beta_2 z)$ and $E_-(z)\exp(-j\beta_2 z)$.

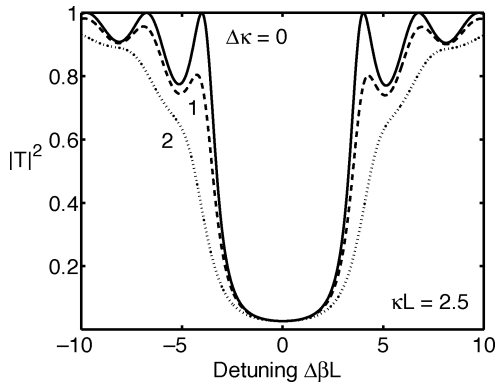

Fig. 2. Transmissivity versus detuning of a linearly tapered linear DFB structure with $\kappa L = 2.5$ for three taper parameters: $\Delta\kappa = 0$, 1, and 2. (for comparison with [7, Fig. 2(a)]).

III. Numerical Examples and Discussion

A. Validity of the Numerical Model

We first check the validity of the proposed numerical model by comparing our calculation with prior reported results. We show the results in both the low- and high-intensity operating regimes, i.e., both linear and nonlinear DFB structures are considered. Two types of nonuniformities, linear taper and linear chirp, are introduced in the DFB structure for comparison. We have observed that the response of an NLDFB structure with 200 periods can well match the prediction of the nonlinear CMT, and the response of a linear DFB structure surely requires even fewer periods to converge. For simplicity, we consider both linear and nonlinear DFB structures operating at the wavelength (in the medium) λ_{B0} with length $L = 200\Lambda$, where $\Lambda = \lambda_{B0}/2$ is the fundamental grating period.

Fig. 2 shows our calculation of the transmissivity $|T|^2$ versus the detuning parameter $\Delta\beta L$ of a linearly tapered linear DFB structure with the average coupling parameter $\kappa L = 2.5$ for three taper parameters: $\Delta\kappa = 0$, 1, and 2. The linear taper is defined to have the form

$$\kappa(z) = \kappa_0\left[1 + \frac{\Delta\kappa\left(z - \frac{L}{2}\right)}{L}\right] \quad (10)$$

over a strictly periodic, uniform DFB structure with the Bragg wavenumber $\beta_{B0} = 2\pi/\lambda_{B0}$, where the linear coupling strength $\kappa(z)$ is related to the perturbation of the refractive

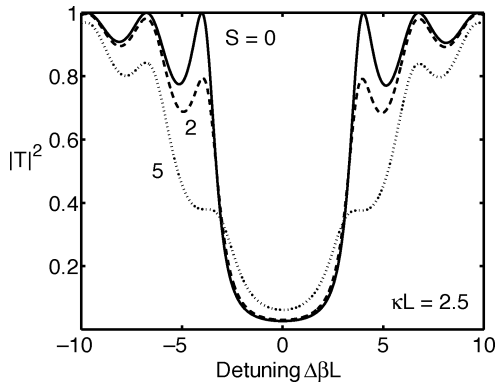

Fig. 3. Transmissivity versus detuning of a linearly chirped Dlinear DFB structure with $\kappa L = 2.5$ for three chirp parameters: $S = 0$, 2, and 5 (for comparison with [7, Fig. 2(b)]).

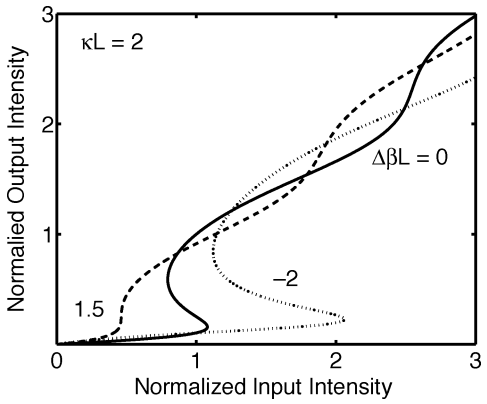

Fig. 4. The normalized output intensity versus the normalized input intensity for a uniform NLDFB structure with $\kappa L = 2$ for three different values of detuning: $\Delta\beta L = 0$, 1.5, and -2 (for comparison with [2, Fig. 1]).

index by $\beta_{B0} n_1(z)/2n_0$. $\Delta\beta$ represents the shift in the operating wavenumber away from β_{B0}. Fig. 3 shows the similar calculation for a linearly chirped DFB structure, again with the average coupling parameter $\kappa L = 2.5$, for three chirp parameters: $S = 0$, 2, and 5. The linear chirp is introduced into the DFB structure such that the Bragg wavenumber varies with the position according to

$$\beta_B(z) = \beta_{B0} + \frac{S\left(z - \frac{L}{2}\right)}{L^2}. \tag{11}$$

Figs. 2 and 3 agree very well with those given in [7] and [9] based on the transfer matrix method calculation. (Our Fig. 3 is to be compared with [7, Fig. 2(b)] in which $S = 0$, 4, and 10 are indicated due to possible difference in the definition of S.) Please note that 10 uniform DFB segments were used to approximate the continuously varying taper or chirp function in [7].

We then consider the uniform NLDFB structure studied by Winful *et al.* [2]. The input and output intensities are normalized to the critical intensity defined in [2] as

$$|E_C|^2 = \frac{4n_0\lambda}{3\pi n^{(2)} L}. \tag{12}$$

We plot in Fig. 4 the normalized output intensity versus the normalized input intensity for three detuing parameters: $\Delta\beta L = 0$, -2, and 1.5, with the coupling parameter $\kappa L = 2$. The results are identical to [2, Fig. 1]. Having confirmed the validity of our proposed method, we can further explore nonuniform NLDFB structures. We will focus on the linearly tapered and linearly chirped NLDFB structures studied in [7].

B. Linearly Tapered NLDFB Structure

As in [7, Fig. 3(a)], the transmission characteristics of the linearly tapered structure of Fig. 2 at zero-detuning ($\Delta\beta L = 0$) are calculated versus the normalized input intensity for $\Delta\kappa = -2$, -1, 0, and 1 and are shown in Fig. 5. Although the curves for $\Delta\kappa = -2$, -1, and 0 are essentially identical to those in [7, Fig. 3(a)] showing that larger input intensity is required for switching for the negative taper, that for $\Delta\kappa = 1$ is obviously different from [7, Fig. 3(a)] in that the hysteresis has not disappeared yet in our result and the throughput efficiency is higher (>0.7 versus ≈0.6 in [7, Fig. 3(a)]). Also, our $\Delta\kappa = 1$ curve shows obvious up-swing near the normalized input intensity of 2.2. Although wider hysteresis width and higher transmission efficiency are seen in our $\Delta\kappa = 1$ result compared with [7, Fig. 3(a)], the introduction of the positive taper still causes shorter hysteresis and lower transmission than the uniform grating case ($\Delta\kappa = 0$), as discussed in [10].

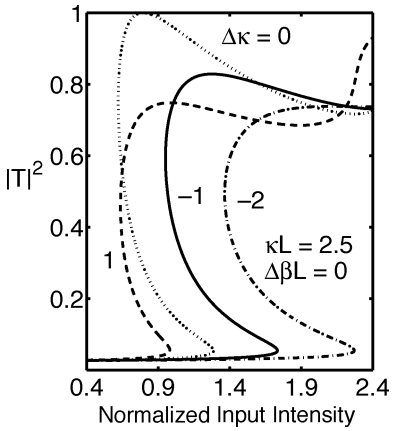

Fig. 5. Transmissivity of a linearly tapered NLDFB structure with $\kappa L = 2.5$ at zero-detuning for four taper parameters: $\Delta\kappa = 0$, 1, -1, and -2 (for comparison with [7, Fig. 3(a)]).

We then consider the edge-tuning case at $\Delta\beta L = 2.5$ as in [7, Fig. 3(b)]. Tuning near the Bragg stop-band edge would lower the switching intensity. Fig. 6 shows our results for $\Delta\kappa = -2$, -1, 0, and 1. Again, the curves for $\Delta\kappa = -2$, -1, and 0 essentially check with those in [7, Fig. 3(a)]. Although the $\Delta\kappa = 0$ case (no taper) shows no hysteresis, it allows up-switching at ≈0.18 normalized input intensity, compared to the intensity of ≈1.3 in Fig. 5. The switching intensity is increased and the transmission efficiency lowered for negative $\Delta\kappa$. Our $\Delta\kappa = 1$ result is quite different from that in [7, Fig. 3(b)]. Our $\Delta\kappa = 1$ curve shows similar slope of switching as the $\Delta\kappa = 0$ one but with lower throughput efficiency, while that in [7, Fig. 3(b)] reveals much worse switching behavior.

C. Linearly Chirped NLDFB Structure

As in [7, Fig. 3(c)], the transmission characteristics of the linearly chirped structure of Fig. 3 at zero-detuning are calculated versus the normalized input intensity for S = -1, 0, 1,

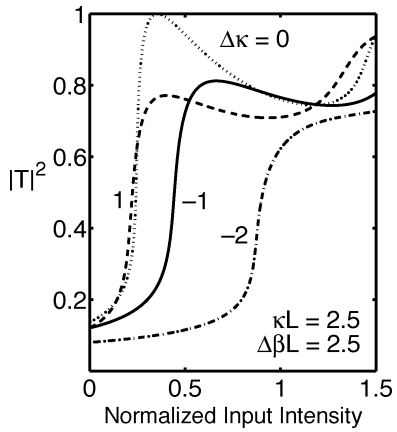

Fig. 6. Transmissivity of a linearly tapered NLDFB structure with $\kappa L = 2.5$ at the edge of Bragg stop-band $\Delta\beta L = 2.5$ for four taper parameters: $\Delta\kappa = 0$, 1, -1, and -2 (for comparison with [7, Fig. 3(b)]).

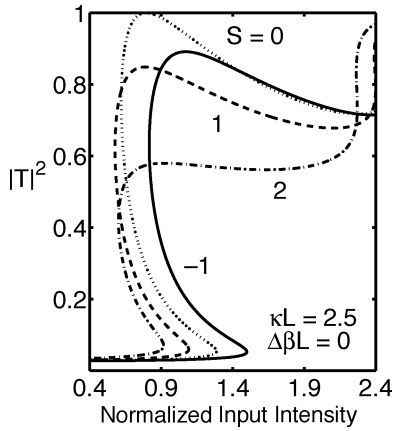

Fig. 7. Transmissivity of a linearly chirped NLDFB structure with $\kappa L = 2.5$ at zero-detuning for four taper parameters: $S = 0$, -1, 1, and 2 (for comparison with [7, Fig. 4(a)]).

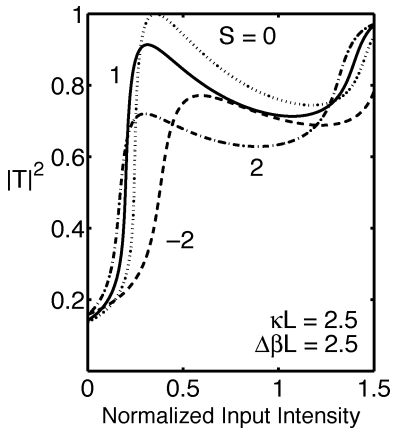

Fig. 8. Transmissivity of a linearly chirped NLDFB structure with $\kappa L = 2.5$ at the edge of Bragg stop-band $\Delta\beta L = 2.5$ for four taper parameters: $S = 0$, -1, 1, and 2 (for comparison with [7, Fig. 4(b)]).

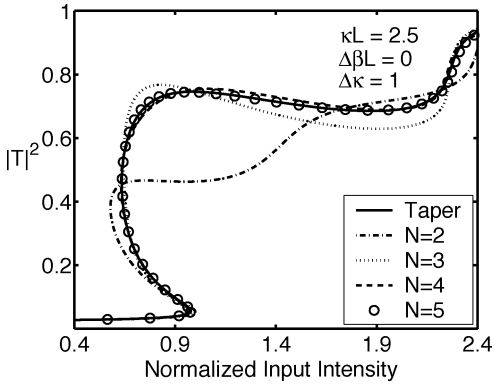

Fig. 9. Transmissivity of a linearly tapered NLDFB structure approximated by a set of N uniform segments with $\kappa L = 2.5$ and $\Delta\kappa = 1$ at zero-detuning for $N = 2-5$. The solid curve is the result of the continuously varying structure.

and 2 and are shown in Fig. 7. Our results essentially reveal the same switching properties as discussed in [7]: negative S values increase the up-switching intensity and positive S values lower both the up-switching intensity and the width of the transmission hysteresis, with the overall transmission efficiency decreased in all the $S \neq 0$ cases. Our $S = 0$ curve agrees with that in [7, Fig. 3(c)], while our $S = -1$ curve shows smaller up-switching intensity ($\approx$1.5 versus $\approx$1.6 in [7, Fig. 3(c)]) and our $S = 1$ and $S = 2$ curves have larger transmission values.

The edge-tuning case at $\Delta\beta L = 2.5$ is also examined for comparing with [7, Fig. 3(d)]. Except that we obtain a little higher transmission efficiency for the $S = 2$ curve, our results shown in Fig. 8 agree with [7, Fig. 3(d)]. The hysteresis is seen to disappear in all curves.

D. Discussion on Segmented Calculation

According to the above discussion related to Figs. 2, 3, and 5–8, we conclude that our calculations agree with those obtained by the transfer matrix method using 10 uniform DFB segments for linear structures and for uniform NLDFB structures ($\Delta\kappa = 0$ and $S = 0$), but show noticeable differences for some linearly tapered and linearly chirped NLDFB structures. Since the connection of uniform segments is only an approximation of the continuously varying perturbation, we would like to examine the convergence property of such segmented calculation for the NLDFB structure based on our numerical approach. Consider the case in Fig. 5 with $\Delta\kappa = 1$. We divide the linearly tapered structure evenly into N segments and replace each segment with a strictly periodic section having a uniform coupling strength equal to the average coupling strength of the original tapered segment. In [7] it was claimed that the validity of the coupled-mode description for the segmented structure requires that the segment length be kept much longer than the period of the DFB structure. Therefore, in our calculations we assume that each segment is composed of 200 periods. The optical response of a uniform segment with 200 periods can well match the prediction of the CMT as we have examined in Fig. 4. The calculated transmission characteristics are shown in Fig. 9 for $N = 2$, 3, 4, and 5. It is seen that the result rapidly converges and the $N = 5$ curve almost matches the solid curve which is obtained without making segmentation. Fig. 10 illustrates similar calculation for the case in Fig. 7 with $S = 1$. Each of the N segments is now replaced by a strictly periodic section having a period equal to the average period of the original chirped segment. Again, the result quickly converges and the difference between

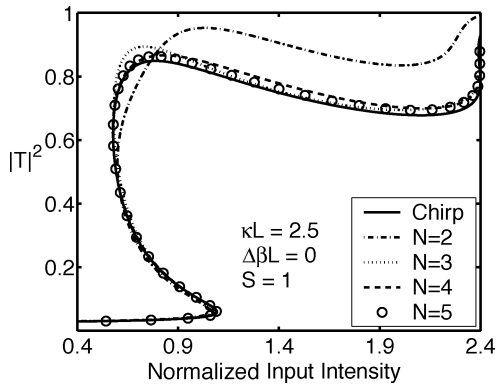

Fig. 10. Transmissivity of a linearly chirped NLDFB structure approximated by a set of N uniform segments with $\kappa L = 2.5$ and $S = 1$ at zero-detuning for $N = 2-5$. The solid curve is the result of the continuously varying structure.

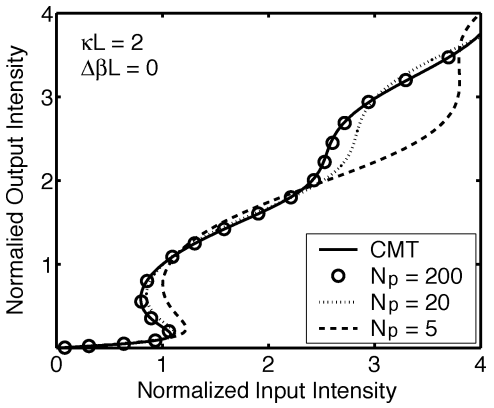

Fig. 12. The normalized output intensity versus the normalized input intensity at zero-detuning for a uniform NLDFB structure composed of N_p periods with $\kappa L = 2$ for $N_p = 5$, 20, and 200. The solid line is the result of the CMT.

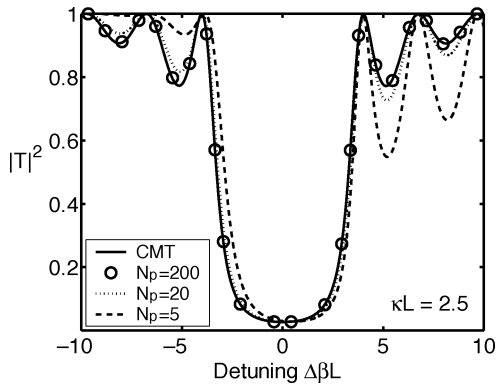

Fig. 11. Transmissivity versus detuning of a uniform linear DFB structure composed of N_p periods with $\kappa L = 2.5$ for $N_p = 5$, 20, and 200. The solid line is the result of the CMT.

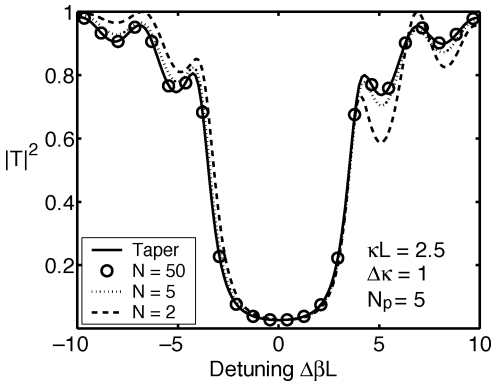

Fig. 13. Transmissivity versus detuning of a linearly tapered linear DFB structure with κL 2.5 and $\Delta\kappa = 1$ approximated by a set of N uniform segments for $N = 2$, 5, and 50. Each uniform segment is composed of N_p periods. The solid line is the result of a sufficiently long and continuously varying structure.

the $N = 5$ curve and the solid curve without using segmented calculation is quite small. Therefore, we confirm the rapid convergence behavior of the transfer matrix treatment and the difference between our results and some of [7, Fig. 3] should not be due to the segmented approximation.

We have also calculated $N > 5$ cases and found that there is no oscillatory solution behavior when the segmentation number is increased, that is, the results are basically indistinguishable from the solid curves in Figs. 9 and 10, under the assumption that each segment is long enough and the perturbation is much smaller than the average index so that the coupled-mode description is correct. It is however interesting to examine the characteristics of the cases in which the individual uniform segments of a long structure after a large-N segmentation possess only few periods. Figs. 11 and 12 show how insufficient periods in a uniform DFB structure would distort its optical response in linear and nonlinear cases, respectively, for the number of periods $N_p = 5$, 20, and 200 based on our numerical approach. The solid lines are the results of the CMT. Note that $\kappa L = 2.5$ in Fig. 11 and $\kappa L = 2$ in Fig. 12 for comparison with Figs. 2 and 4, respectively. With decreasing L or N_p, and thus increasing κ, the prediction of the CMT reveals increasing inaccuracy. We now examine the accuracy of the segmented calculation for the nonuniform DFB structure with insufficient periods, say, 5 periods ($N_p = 5$) in each segment. Consider the linearly tapered

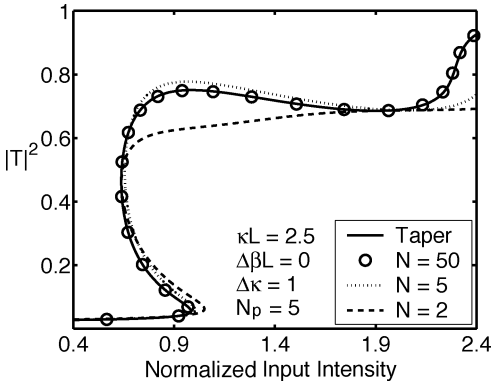

Fig. 14. Transmissivity at zero-detuning of a linearly tapered NLDFB structure with $\kappa L = 2.5$ and $\Delta\kappa = 1$ approximated by a set of N uniform segments for $N = 2$, 5, and 50. Each uniform segment is composed of N_p periods. The solid line is the result of a sufficiently long and continuously varying structure.

linear structure with $\kappa L = 2.5$ and $\Delta\kappa = 1$ in Fig. 2, but approximated by N uniform segments. The $|T|^2$ versus $\Delta\beta L$ results for $N = 2$, 5, and 50 obtained using our numerical approach are shown in Fig. 13, where the solid line represents the result of a sufficiently long and continuously varying structure without segmentation, or the $\Delta\kappa = 1$ line in Fig. 2. Note that

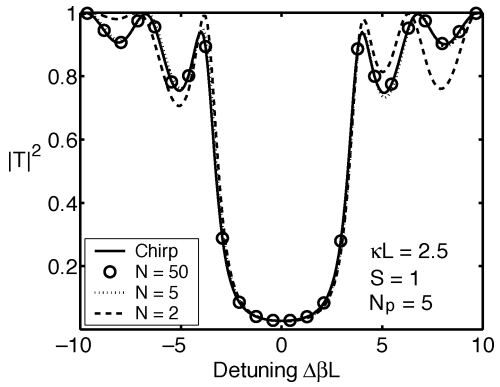

Fig. 15. Transmissivity versus detuning of a linearly chirped linear DFB structure with $\kappa L = 2.5$ and $S = 1$ approximated by a set of N uniform segments for $N = 2$, 5, and 50. Each uniform segment is composed of N_p periods. The solid line is the result of a sufficiently long and continuously varying structure.

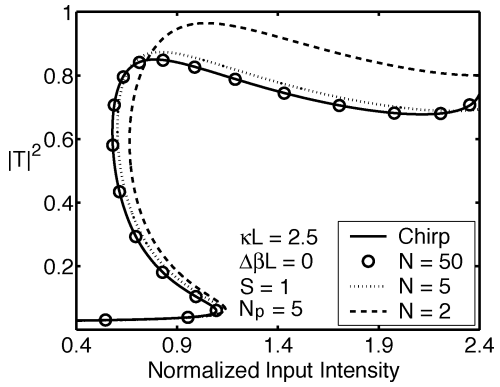

Fig. 16. Transmissivity at zero-detuning of a linearly chirped NLDFB structure with $\kappa L = 2.5$ and $S = 1$ approximated by a set of N uniform segments for $N = 2$, 5, and 50. Each uniform segment is composed of N_p periods. The solid line is the result of a sufficiently long and continuously varying structure.

for a given N, the length of the structure is $NN_p\Lambda = 5N\Lambda$, but the average coupling parameter $\kappa L = 2.5$ is the same. It is seen that as long as N is large enough, or the total number of periods NN_p is large enough, the segmented calculation matches that without segmentation even though each segment contains only 5 periods. Similar conclusion is obtained for the linearly tapered nonlinear structure ($\kappa L = 2.5$, $\Delta\beta L = 0$, and $\Delta\kappa = 1$), the linearly chirped linear structure ($\kappa L = 2.5$ and $S = 1$), and the linearly chirped nonlinear structure ($\kappa L = 2.5$, $\Delta\beta L = 0$, and $S = 1$), as shown in Figs. 14, 15, and 16, respectively, where Figs. 14 and 16 are for comparison with Figs. 9 and 10, respectively.

IV. Conclusion

In this paper we have adopted a simple numerical approach for the analysis of nonuniform NLDFB structures. The method was previously proposed for calculating the input-intensity dependence of the reflectivity and transmissivity of a nonlinear dielectric slab for both transverse-electric (TE) and transverse-magnetic (TM) obliquely incident plane electromagnetic waves [8]. The method is powerful in that the medium considered can have an arbitrary linear permittivity profile transverse to the slab interface and arbitrary nonlinear dependence of the permittivity on the electric field of the wave. We have demonstrated that our calculation of the continuous-wave optical response of a strictly periodic NLDFB structure agrees perfectly with Winful *et al.*'s analytic results. We then consider linearly tapered and linearly chirped NLDFB structures as studied by Radic *et al.* [7] as numerical examples. A generalized transfer matrix by approximating the continuously varying nonuniform NLDFB structure with a set of strictly periodic, uniform segments was used in [7]. Although our results agree with those of [7] for the linear DFB cases, differences in the prediction of the transmission bistability characteristics have been observed in some of the NLDFB structures. We have examined using our numerical approach the possible difference between segmented calculation and continuously varying structure analysis and found that the former quickly converges to the latter as the number of segments increases.

References

[1] M. Okuda and K. Onaka, "Bistability of optical resonator with distributed Bragg-reflectors by using Kerr effect," *Jpn. J. Appl. Phys.*, vol. 16, pp. 769–773, 1977.

[2] H. G. Winful, J. H. Marburger, and E. Gamire, "Theory of bistability in nonlinear distributed feedback structures," *Appl. Phys. Lett.*, vol. 35, pp. 379–381, 1979.

[3] J. He, M. A. Dupertuis, D. Martin, F. M. Genoud, C. Rolland, and A. J. S. Thorpe, "All-optical bistable switching and signal regeneration in a semiconductor layered distributed-feedback/Fabry–Perot structure," *Appl. Phys. Lett.*, vol. 63, pp. 866–868, 1992.

[4] N. D. Sankey, D. F. Prelewitz, and T. G. Brown, "All-optical switching in a nonlinear periodic-waveguide structure," *Appl. Phys. Lett.*, vol. 60, pp. 1427–1429, 1992.

[5] C. J. Herbert and M. S. Malcuit, "Optical bistability in nonlinear periodic structures," *Opt. Lett.*, vol. 18, pp. 1783–1785, 1993.

[6] G. Li, J. A. Tobin, and D. D. Denton, "Excitation of nonlinear guided waves in Kerr-type media using chirped and tapered gratings," *J. Opt. Soc. Amer. B*, vol. 83, pp. 2290–2297, 1993.

[7] S. Radic, N. George, and G. P. Agrawal, "Analysis of nonuniform nonlinear distributed feedback structures: generalized transfer matrix method," *IEEE J. Quantum Electron.*, vol. 31, pp. 1326–1336, May 1995.

[8] H.-C. Chang and L. C. Chen, "Simple numerical approach for determining the optical response of a nonlinear dielectric film for both TE and TM waves," *Phys. Rev. B*, vol. 43, pp. 9436–9441, 1991.

[9] M. Yamada and K. Sakuda, "Analysis of almost-periodic distributed feedback slab waveguides via a fundamental matrix approach," *Appl. Opt.*, vol. 26, pp. 3474–3478, 1987.

[10] G. Assanto, R. Zanoni, and G. I. Stegeman, "Effects of taper in nonlinear distributed feedback gratings," *J. Mod. Opt.*, vol. 35, pp. 871–883, 1988.

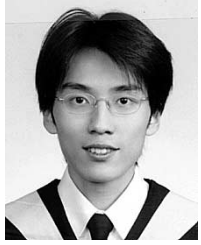

Chu-Sheng Yang was born in Taipei, Taiwan, R.O.C., on November 1, 1980. He received the B.S. degree in electrical engineering from National Taiwan University, Taipei, R.O.C., in 2002.

He is currently a Research Assistant with the Computational Electromagnetics Laboratory within the same University, where he is conducting research on the problems of optical switching and bistability, optical tristability, nonlinear periodic structures, etc.

Yen-Chung Chiang was born in Hualien, Taiwan, on March 10, 1970. He received the B.S., M.S., and Ph.D. degrees in electrical engineering from National Taiwan University, Taipei, Taiwan, R.O.C., in 1992, 1994, and 2002, respectively. His Ph.D. dissertation was on the numerical techniques of mode solvers for optical waveguide structures.

He is now with the VIA Technologies Inc., Taipei, where he is currently a Senior Engineer in the Research and Development Division, Mixed-signal/RF department. His research interests include numerical methods for analyzing guided wave structures and photonic crystal structures.

Hung-Chun Chang (S'78–M'83–SM'00) was born in Taipei, Taiwan, R.O.C., on February 8, 1954. He received the B.S. degree from National Taiwan University, Taipei, in 1976, and the M.S. and Ph.D. degrees from Stanford University, Stanford, CA, in 1980 and 1983, respectively, all in electrical engineering.

From 1978 to 1984, he was with the Space, Telecommunications, and Radioscience Laboratory of Stanford University. In August 1984, he joined the faculty of the Electrical Engineering Department of National Taiwan University, where he is currently a Professor. He served as Vice-chairman of the Electrical Engineering Department from 1989 to 1991, and Chairman of the newly established Graduate Institute of Electro-Optical Engineering from 1992 to 1998. His current research interests include the theory, design, and application of guided-wave structures and devices for fiber optics, integrated optics, optoelectronics, and microwave and millimeter-wave circuits.

Dr. Chang is a member of Sigma Xi, Phi Tau Phi, the Chinese Institute of Engineers, the Photonics Society of Chinese-Americans, the Optical Society of America, the Electromagnetics Academy, and China/SRS (Taipei) National Committee (a Standing Committee member during 1988–1993) and Commission H of U.S. National Committee of the International Union of Radio Science (URSI). In 1987, he was among the recipients of the Young Scientists Award at the URSI XXI General Assembly. In 1993, he was one of the recipients of the Distinguished Teaching Award sponsored by the Ministry of Education of the Republic of China.